
Propagation of Love Waves Through an Irregular Surface of a Layered Poroelastic Rock Structure

Anil Negi^{1,*} and Saurabh Kapoor^{2,*}

¹*Department of Mathematics, School of Advanced Sciences, VIT-AP, University,
Andhra Pradesh, India*

²*Department of Education in Science and Mathematics, Regional Institute of
Education (NCERT), Bhubneshwar, Odisha, India*

E-mail: negi.anil3@gmail.com; saurabh09.ncert@gmail.com

**Corresponding Author*

Received 21 April 2023; Accepted 26 May 2023;

Publication 31 July 2023

Abstract

The present study adduces the dynamic properties of the propagating Love waves passing through the irregular upper surface of transversely isotropic poroelastic structure. The dispersion relation for scattered Love waves in a closed form and induced reflected displacement caused by scattering of waves have been derived. The impact of the porosity of the upper layer and half-space on the phase velocity and also on the reflected displacement have also been studied. The porosity of both upper layer and half-space have significant effect on the phase velocity of Love waves. Moreover, the nature of induced reflected displacement with the change in vertical irregularity parameter is also analyzed. The vertical irregularity parameter (associated with the vertical depth of irregularity) has escalating impact on the induced

Journal of Graphic Era University, Vol. 11.2, 153–176.

doi: 10.13052/jgeu0975-1416.1123

© 2023 River Publishers

reflected displacement. The comparative analysis of reflected displacement in three distinct scenarios of vertical irregularity has also been done.

Keywords: Poroelastic, phase velocity, porosity, and reflected displacement, Love waves.

1 Introduction

The study of Love waves propagation has attracted many researchers of geology, civil engineering, earthquake engineering, and geophysics etc. all over the world. The observation of the Love waves propagation is fruitful in diverse areas viz. material characterization, seismology and non-destructive testing (NDT) (Baroudi, 2018). Poroelastic rocks are generally found in the uppermost earth's crust. The different processes like alignment of crystals, layering of sedimentary beds, and orientation of grains can cause the anisotropy in the poroelastic rocks. The anisotropy of rocks can play a vital role to understand the structural strength affected by seismic waves. The anisotropic medium in which axis of symmetry is vertical is called vertical transversely isotropic medium. This type of medium exhibits the uniform properties in a horizontal plane but having different properties in the direction of the vertical axis. The layered rocks (viz. sandstones) show vertical transversely isotropic behavior. Some physical phenomena such as weathering, external loads, etc. can cause the upper irregular surface in the poroelastic rocks. As the interaction of irregularity in upper surface and Love waves occurs, the destructive impact due to Love waves increases. Therefore, it is important to study the Love waves propagation in the irregular poroelastic rock structures.

The fundamental equation for the Love waves which represents the dispersion characteristics of Love waves in the isotropic elastic structure has been provided by Love (1944). The investigations on the elastic waves propagating in the fluid-saturated porous solid have been accomplished by Biot (1962). The propagation of shear waves in an irregular anisotropic structure has been investigated by Chattopadhyay and Pal (1982). Chattopadhyay and De (1983) explore the propagation characteristics of Love waves in a porous medium with irregular interface. Sharma (2004) studied the propagation of plane harmonic waves in an anisotropic poroelastic and permeable rock. The scattering characteristics for the propagation of Love waves in

a layered isotropic elastic structure have been examined by Wolf (1970). Negi and Singh (2019) investigated the propagation characteristics of Love waves through upper irregular surface of layered and irregular piezoelectric structure.

After analyzing the available literatures, it is found that several researchers investigated the Love waves propagation in a viscoelastic, isotropic and piezoelectric layered structures. But, the analysis of Love waves propagation in the transversely isotropic poroelastic layered rock material structure having irregular surface is not done yet. The behaviors of anisotropy parameter and porosity on the phase velocity of scattered Love waves are not studied till date. These facts serve as motivation for the authors to study the dynamic behavior of Love waves propagation in a poroelastic layered rock material structure having irregular surface has been done through present study.

The closed expression for the dispersion relation associated with Love waves interacting with the upper irregular surface of a layered poroelastic rock material structure has been obtained. The influences of porosity and anisotropic parameters associated with upper poroelastic rock layer on the scaled phase velocity are analyzed. Reflected displacement component caused by waves scattering is also obtained analytically. The effectuality of anisotropic parameter and vertical irregularity parameter corresponds to the upper poroelastic rock layer on the component of reflected displacement component is studied for different shapes of irregularity in upper surface.

2 Formulation of the Problem

Let us consider a layered poroelastic rock structure having layer of thickness H . The configuration of this medium (shown in Figure 1) has been considered in such a way that the propagation of Love waves is along the direction of x -axis, and z -axis being assumed to be oriented vertically downwards. Moreover, $z = 0$ represents the interface that connects the upper layer and lower half space of the considered rock medium.

The irregularity in the upper poroelastic rock layer can have the following representation (Wolf, 1970; Chattopadhyay et al., 2010; Negi and Singh, 2019)

$$z = z_B = -H + bh_0(x), \quad (1)$$

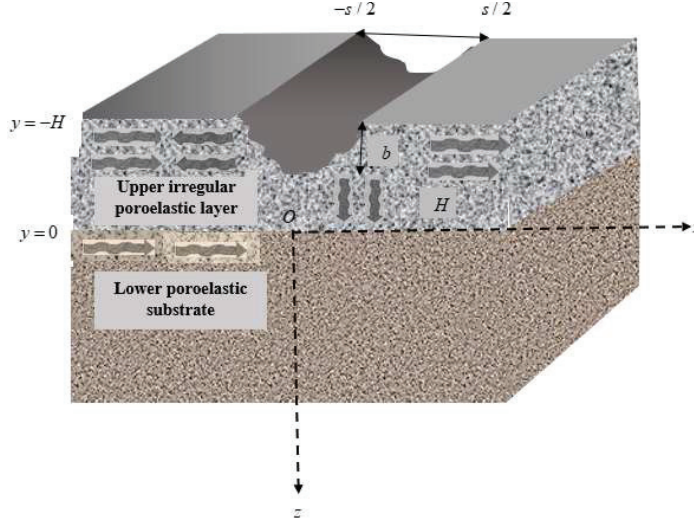


Figure 1 Geometry of the problem.

where $h_0(x)$ can be represented as

$$h_0(x) = \begin{cases} 0 & \text{for } x \leq -\frac{s}{2} \text{ and } x \geq \frac{s}{2} \\ f_0(x), & \text{for } -\frac{s}{2} \leq x \leq \frac{s}{2}. \end{cases} \quad (2)$$

the width of the irregularity in the upper layer is indicated by the variable ‘ s ’; $b(=1)$ indicates the magnitude (or size) of the irregularity in upper rock surface, and $f_0(x)$ corresponds to the shape of the irregularity in the upper poroelastic surface.

The equations describing the propagation of Love waves in the direction of x -axis and cause displacement in the direction of y -axis are given by (Love, 1944; Negi and Singh, 2019)

$$\left. \begin{aligned} u_1 = w_1 = 0, \quad v_1 = v_1(x, z, t), \quad \text{and } U_1 = W_1 = 0, \quad V_1 = V_1(x, z, t), \\ u_2 = w_2 = 0, \quad v_2 = v_2(x, z, t), \quad \text{and } U_2 = W_2 = 0, \quad V_2 = V_2(x, z, t) \end{aligned} \right\} \quad (3)$$

where (u_k, v_k, w_k) and (U_k^*, V_k^*, W_k^*) represent displacement components correspond to the solid and fluid phases, and refer to the directions of x -axis, y -axis, and z -axis respectively; $k = 1$ is related with the upper poroelastic rock layer while $k = 2$ represents the lower half-space in the studied poroelastic rock medium.

The stress-strain relations for Love waves propagation in poroelastic medium can be written as (Biot, 1956, 1962)

$$\left. \begin{aligned} \tau_{xx} &= c_{11}\varepsilon_{xx} + c_{12}\varepsilon_{yy} + c_{13}\varepsilon_{zz} + M \left(\frac{\partial U}{\partial x} + \frac{\partial V}{\partial y} + \frac{\partial W}{\partial z} \right), \\ \tau_{yy} &= c_{12}\varepsilon_{xx} + c_{11}\varepsilon_{yy} + c_{13}\varepsilon_{zz} + M \left(\frac{\partial U}{\partial x} + \frac{\partial V}{\partial y} + \frac{\partial W}{\partial z} \right), \\ \tau_{zz} &= c_{13}\varepsilon_{xx} + c_{13}\varepsilon_{yy} + c_{33}\varepsilon_{zz} + J \left(\frac{\partial U}{\partial x} + \frac{\partial V}{\partial y} + \frac{\partial W}{\partial z} \right), \\ \tau_{xy} &= \tau_{yx} = c_{66}\varepsilon_{xy}, \quad \tau_{zy} = \tau_{yz} = c_{44}\varepsilon_{yz}, \quad \tau_{zx} = \tau_{xz} = c_{44}\varepsilon_{zx}, \\ \tau &= D \left(\frac{\partial U}{\partial x} + \frac{\partial V}{\partial y} + \frac{\partial W}{\partial z} \right) + M\varepsilon_{xx} + M\varepsilon_{yy} + J\varepsilon_{zz}, \end{aligned} \right\} \quad (4)$$

where $\tau_{ij}(i, j = x, y, z)$ denote the stress components; $\varepsilon_{ij} = \frac{1}{2}(u_{i,j} + u_{j,i})$ represent the strain components; c_{ij} , M , and J are the elastic constants for the poroelastic materials and τ denotes the stress acting on the phase of fluid.

The equations of motion for the poroelastic medium with transversely isotropy can be expressed as (Biot, 1956; Biot, 1962)

$$\left. \begin{aligned} \frac{\partial}{\partial x}\tau_{xx} + \frac{\partial}{\partial y}\tau_{xy} + \frac{\partial}{\partial z}\tau_{xz} &= \frac{\partial^2}{\partial t^2}(\rho_{11}u + \rho_{12}U), \\ \frac{\partial}{\partial x}\tau_{yx} + \frac{\partial}{\partial y}\tau_{yy} + \frac{\partial}{\partial z}\tau_{yz} &= \frac{\partial^2}{\partial t^2}(\rho_{11}v + \rho_{12}V), \\ \frac{\partial}{\partial x}\tau_{zx} + \frac{\partial}{\partial y}\tau_{zy} + \frac{\partial}{\partial z}\tau_{zz} &= \frac{\partial^2}{\partial t^2}(\rho_{11}w + \rho_{12}W), \\ \frac{\partial \tau}{\partial x} &= \frac{\partial^2}{\partial t^2}(\rho_{12}u + \rho_{22}U), \\ \frac{\partial \tau}{\partial y} &= \frac{\partial^2}{\partial t^2}(\rho_{12}v + \rho_{22}V), \\ \frac{\partial \tau}{\partial z} &= \frac{\partial^2}{\partial t^2}(\rho_{12}w + \rho_{22}W), \end{aligned} \right\} \quad (5)$$

where ρ_{11} is inertial coefficient associated with the mass density for the solid phase; ρ_{22} signifies to the inertial coefficient associated with the mass density

of fluid phase; ρ_{12} is inertial coefficient associated with the mass density for the coupling between the fluid and solid phases.

The inertial coefficients ρ_{11} , ρ_{12} and ρ_{22} together with $\rho_{11} > 0$, $\rho_{22} > 0$, and $\rho_{12} \leq 0$ can be written as (Biot, 1956; Biot, 1962)

$$\rho_{11}\rho_{22} - \rho_{12}^2 > 0, \text{ and } \rho = \rho_{11} + 2\rho_{12} + \rho_{22} = \rho_s + \phi(\rho_s - \rho_f) \quad (6)$$

where ρ represents the total mass density for the studied medium and ϕ denotes the porosity of the studied medium; ρ_f and ρ_s denote the densities for the fluid and solid phases respectively.

With the help of Equation (3) and stress-strain relations indicated by Equation (4), the equations of motion in Equation (5) yields

$$c_{44} \frac{\partial^2 v_k}{\partial x^2} + c_{66} \frac{\partial^2 v_k}{\partial z^2} = \rho' \frac{\partial^2 v_k}{\partial t^2}, \quad (7)$$

where

$$\rho' = \left(\rho_{11} - \frac{(\rho_{12})^2}{\rho_{22}} \right).$$

The simplification of Equation (7) provides

$$\frac{\partial^2 v_k}{\partial x^2} + \frac{1}{\gamma^2} \frac{\partial^2 v_k}{\partial z^2} = \frac{1}{\beta^2} \frac{\partial^2 v_k}{\partial t^2}, \quad (8)$$

In view of harmonic variation of time i.e. $e^{i\omega t}$ for the displacement component, we have (Wolf, 1970; Chattopadhyay et al, 2010; Negi and Singh, 2019)

$$v_k(x, z, t) = V_k(x, z)e^{i\omega t}, \quad (9)$$

where the symbol ω denotes the angular frequency; $k = 1$ related with the upper poroelastic rock layer while $k = 2$ is linked to the half-space of the poroelastic rock medium.

In view of Equations (8) and (9), we have

$$\frac{\partial^2 V_1}{\partial x^2} + \frac{1}{\gamma_1^2} \frac{\partial^2 V_1}{\partial z^2} + K_1^2 V_1 = 0, \quad (10)$$

$$\frac{\partial^2 V_2}{\partial x^2} + \frac{1}{\gamma_2^2} \frac{\partial^2 V_2}{\partial z^2} + K_2^2 V_2 = 0, \quad (11)$$

where γ_1^2 , γ_2^2 , K_1^2 , and K_2^2 are provided in the **Appendix**.

Boundary Conditions

- (i) For the upper free surface at $z = -H + bh_0(x)$ where $(h'_0 = \frac{dh_0}{dx})$, the traction free boundary condition can be written as

$$\tau_{yz}^1 - \gamma_1^2 bh'_0 \tau_{yx}^1 = 0. \quad (12)$$

- (ii) At the interface $z = 0$, the equations for the continuity boundary conditions can be expressed as

$$v_1 = v_2, \quad (13)$$

$$\tau_{yz}^1 = \tau_{yz}^2. \quad (14)$$

3 Problem Solution

With the help of Equations (10)–(11), the expression for the solution for the incident wave field may be expressed as (Wolf, 1970; Chattopadhyay et al., 2010)

$$v_{1,in} = A \cos \gamma_1 s_1 (z + H) e^{-i\mu x}, \quad (15)$$

$$v_{2,in} = B e^{-\gamma_2 s_2 z} e^{-i\mu x}, \quad (16)$$

where $s_1^2 = K_1^2 - \mu^2$, $s_2^2 = K_2^2 - \mu^2$; $\mu = \frac{\omega}{c_{ph}}$ represents the angular wave number for the incident wave field; c_{ph} signifies the phase velocity of Love waves; A and B are the arbitrary coefficients correspond to the incident wave field.

In the similar manner, Equations (10)–(11) provide the expression for solution for scattered wave field as (Wolf, 1970; Chattopadhyay et al., 2010)

$$v_{1,scatt} = \int_c \{C(v) e^{-i\gamma_1 \xi_1 z} + D(v) e^{i\gamma_1 \xi_1 z}\} e^{-ivx} dv, \quad (17)$$

$$v_{2,scatt} = \int_c E(v) e^{-\gamma_2 \xi_2 z} e^{-ivx} dv, \quad (18)$$

where $\xi_1^2 = K_1^2 - v^2$, $\xi_2^2 = v^2 - K_2^2$; $C(v)$, $D(v)$ and $E(v)$ represent arbitrary coefficients associated with the scattered wave field; $v = \frac{\omega}{c_{ph}}$ indicates the angular wave number; c_{ph} denotes the phase velocity. $v_{k,in}$ and $v_{k,scatt}$ denote the non-vanishing component for the displacement for the incident wave field and the wave field associated with the scattering respectively; $k = 1$ is related

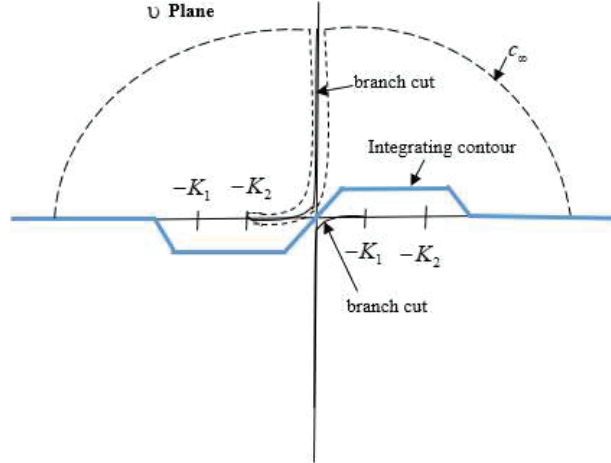


Figure 2 Contour integral in v -plane.

with the upper poroelastic rock layer while $k = 2$ is associated with the lower half space.

The contour integral associated with the scattered wave field has been illustrated by Figure 2 as (Wolf, 1970; Chattopadhyay et al., 2010)

With the help of Equations (15)–(18), the component for the total displacement associated with Love waves propagation can be represented as

$$v_1 = v_{1,in} + v_{1,scatt} = A \cos \gamma_1 s_1 (z + H) e^{-i\mu x} + \int_c \{C(v) e^{-i\gamma_1 \xi_1 z} + D(v) e^{i\gamma_1 \xi_1 z}\} e^{-ivx} dv, \quad (19)$$

$$v_2 = v_{2,in} + v_{2,scatt} = B e^{-\gamma_2 s_2 z} e^{-i\mu x} + \int_c E(v) e^{-\gamma_2 \xi_2 z} e^{-ivx} dv. \quad (20)$$

The boundary condition (13) together with Equations (19)–(20) provide

$$A \cos \gamma_1 s_1 H = B, \quad (21)$$

$$C(v) + D(v) = E(v). \quad (22)$$

In view of Equations (20) and (22), we get

$$v_2 = A \cos \gamma_1 s_1 H e^{-\gamma_2 s_2 z} e^{-i\mu x} + \int_c E(v) e^{-\gamma_2 \xi_2 z} e^{-ivx} dv. \quad (23)$$

In view of Equations (19) and (23), Equation (14) provides

$$C(v) - D(v) = \frac{1}{\lambda} E(v), \quad (24)$$

where

$$\lambda = \frac{i\gamma_1 \xi_1 c_{66}^1}{\gamma_2 \xi_2 c_{66}^2}.$$

From Equations (22) and (24), we have

$$E(v) = C(v) \left(\frac{2\lambda}{\lambda + 1} \right) \quad \text{and} \quad D(v) = C(v) \left(\frac{\lambda - 1}{\lambda + 1} \right). \quad (25)$$

With the help of Equation (25), Equations (19) and (23) yield

$$v_1 = A \cos \gamma_1 s_1 (z + H) e^{-i\mu x} + \int_c \frac{2C}{1 + \lambda} \{ \lambda \cos \gamma_1 \xi_1 z - i \sin \gamma_1 \xi_1 z \} e^{-ivx} dv, \quad (26)$$

$$v_2 = A \cos \gamma_1 s_1 H e^{-\gamma_2 s_2 z} e^{-i\mu x} + \int_c \frac{2C}{1 + \lambda} \{ \lambda e^{-\gamma_2 \xi_2 z} \} e^{-ivx} dv. \quad (27)$$

The surface irregularity is assumed to be very small (i.e. $b \ll 1$) in the studied poroelastic layer which provides

$$C(v) = bC_1(v), \quad \sin \theta_1 b h_0 \cong \theta_1 b h_0, \quad \cos \theta_1 b h_0 \cong 1 \quad (b \ll 1). \quad (28)$$

Equations (26)–(28) together with Equation (12) provide

$$A[-i\gamma_1 \mu h'_0 + \gamma_1 s_1^2 h_0] e^{-i\mu x} + \int_c \left(\frac{2}{1 + \lambda} \right) C_1(v) (i \cos \gamma_1 \xi_1 H - \lambda \sin \gamma_1 \xi_1 H) \xi_1 e^{-ivx} dv = 0. \quad (29)$$

The inversion of Equation (29) provides

$$C_1(v) = \frac{A(\lambda + 1)}{4\pi(i \cos \gamma_1 \xi_1 H - \lambda \sin \gamma_1 \xi_1 H) \xi_1} \times \int_{-\infty}^{\infty} [i\gamma_1 \mu h'_0 - \gamma_1 s_1^2 h_0] e^{iy(v-\mu)} dy. \quad (30)$$

In view of Equations (26), (27) and (30), we get

$$v_1 = A \cos \gamma_1 s_1 (z + H) e^{-i\mu x} + b \int_{-\infty}^{\infty} \frac{A}{2\pi} [i\gamma_1 \mu h'_0 - \gamma_1 s_1^2 h_0] e^{-i\mu y} \\ \times \int_c \frac{\{\lambda \cos \gamma_1 \xi_1 z - i \sin \gamma_1 \xi_1 z\} e^{i\nu y - i\nu x}}{(i \cos \gamma_1 \xi_1 H - \lambda \sin \gamma_1 \xi_1 H) \xi_1} d\nu dy, \quad (31)$$

$$v_2 = A \cos \gamma_1 s_1 H e^{-i\mu x} e^{-\gamma_2 \xi_2 z} + b \int_{-\infty}^{\infty} \frac{A}{2\pi} [i\gamma_1 \mu h'_0 - \gamma_1 s_1^2 h_0] e^{-i\mu y} \\ \times \int_c \frac{\lambda e^{-\gamma_2 \xi_2 z} e^{i\nu y - i\nu x}}{(i \cos \gamma_1 \xi_1 H - \lambda \sin \gamma_1 \xi_1 H) \xi_1} d\nu dy. \quad (32)$$

On rearranging Equations (31)–(32), we get

$$v_1 = A \cos \gamma_1 s_1 (y + H) e^{-i\mu x} \\ + \frac{Ab}{2\pi} \int_{-\infty}^{\infty} [i\gamma_1 \mu h'_0 - \gamma_1 s_1^2 h_0] e^{-i\mu y} dy \times \int_c \Gamma_0(v) dv, \quad (33)$$

$$v_2 = A \cos \gamma_1 \xi_1 H e^{-i\mu x} \\ + \frac{Ab}{2\pi} \int_{-\infty}^{\infty} [i\gamma_1 \mu h'_0 - \gamma_1 s_1^2 h_0] e^{-i\mu y} dy \times \int_c \Gamma_{00}(v) dv. \quad (34)$$

where $\Gamma_0(v)$ and $\Gamma_{00}(v)$ are presented in the given **Appendix**.

The singularities in the contour integrals (31)–(32) provide

$$(i \cos \gamma_1 \xi_1 H - \lambda \sin \gamma_1 \xi_1 H) \xi_1 = 0. \quad (35)$$

On substituting γ_1 , ξ_1 and λ into Equation (35), we get

$$\tan \left(\frac{\sqrt{c_{44}^1}}{\sqrt{c_{66}^1}} \sqrt{(K_1^2 - v^2)} \right) H = \frac{\frac{\sqrt{c_{44}^2}}{\sqrt{c_{66}^2}} c_{66}^2 \sqrt{(v^2 - K_2^2)}}{\frac{\sqrt{c_{44}^1}}{\sqrt{c_{66}^1}} c_{66}^1 \sqrt{(K_1^2 - v^2)}}. \quad (36)$$

Equation (36) adduces the generalized periodic wave equation associated with the Love waves propagation in the studied poroelastic medium. In view of Figure 2, it has been seen that Equation (36) has M roots, where M denotes the integral multiple of $[\{(K_1^2 - K_2^2) \frac{H}{\pi}\} + 1]$ (Wolf, 1970).

In view of Figure 2, the contour integrals in Equations (33)–(34) can be expressed as

$$\int_c \Gamma_0(v)dv = 2\pi i \sum \text{Res } \Gamma_0(v) - \int_{\text{Branch line}} \Gamma_0(v)dv - \int_{c_\infty} \Gamma_0(v)dv, \quad (37)$$

$$\int_c \Gamma_{00}(v)dv = 2\pi i \sum \text{Res } \Gamma_{00}(v) - \int_{\text{Branch line}} \Gamma_{00}(v)dv - \int_{c_\infty} \Gamma_{00}(v)dv. \quad (38)$$

The contour integrals $\int_c \Gamma_0(v)dv$ and $\int_c \Gamma_{00}(v)dv$ have the residues in the form of following expressions

$$\text{Res}(\Gamma_0(v_m)) = \frac{\cos \gamma_1 \xi_{1m}(z + H)e^{iv_m(y-x)}}{\gamma_1 v_m H}, \quad (39)$$

$$\text{Res}(\Gamma_{00}(v_m)) = \frac{\cos \gamma_1 \xi_{1m} H e^{-\gamma_2 \xi_{2m} z} e^{iv_m(y-x)}}{\gamma_1 v_m H}, \quad (40)$$

where $\xi_{km} (k = 1, 2)$.

By adopting the technique given by Sezawa (1935), Equations (37)–(38) which represent the contour integrals are solved. To solve the above-mentioned contour integrals, the contour having branch cuts as K_1 and K_2 that contain real axis as well as semi-circle having infinite radius in the upper half-plane was assumed. The impact of the Love waves propagation is considered around the uppermost surface of the studied poroelastic medium. In the contour integrals (37)–(38), the branch line integrals contain the term of $1/z^{3/2}$, which leads to the negligible values of branch line integrals in front of the residue term when the point of study tends to far from the irregular portion of the upper poroelastic layer. Furthermore, the portion of contour integrals associated with the arc at the infinite point attains zero value for the higher x and y . In view of this, Equations (37)–(38) together with Equations (39)–(40) provide the following expressions for the region $y > x$ and $\text{Re}(v_m) < 0$

$$\int_c \Gamma_0(v)dv = 2\pi i \sum_{m=1}^M \frac{\cos \gamma_1 \xi_{1m}(z + H)e^{iv_m(y-x)}}{\gamma_1 v_m H}, \quad (41)$$

$$\int_c \Gamma_{00}(v)dv = 2\pi i \sum_{m=1}^M \frac{\cos \gamma_1 \xi_{1m} H e^{-\gamma_2 \xi_{2m} z} e^{iv_m(y-x)}}{\gamma_1 v_m H}. \quad (42)$$

In a similar manner, for $\text{Re}(v_m) > 0$ and $y < x$, we get

$$\int_c \Gamma_0(v) dv = -2\pi i \sum_{m=1}^M \frac{\cos \gamma_1 \xi_{1m}(z+H) e^{iv_m(y-x)}}{\gamma_1 v_m H}, \quad (43)$$

$$\int_c \Gamma_{00}(v) dv = -2\pi i \sum_{m=1}^M \frac{\cos \gamma_1 \xi_{1m} H e^{-\gamma_2 \xi_{2m} z} e^{iv_m(y-x)}}{\gamma_1 v_m H}. \quad (44)$$

With the help of Equations (41)–(44), Equations (33)–(34) provide

$$\begin{aligned} v_1 = & A \cos \gamma_1 s_1 (z+H) e^{-i\mu x} - iAb \sum_{m=1}^M \frac{\cos \gamma_1 \xi_{1m}(z+H)}{v_m H} \\ & \times \left\{ e^{-i\mu y} \int_{-\infty}^x (i\mu h'_0 - s_1^2 h_0) \times e^{iv_m(y-x)} dy \right. \\ & \left. + e^{i\mu y} \int_x^{\infty} (i\mu h'_0 - s_1^2 h_0) e^{-i\mu y} \times e^{-iv_m(y+x)} dy \right\}, \quad (45) \end{aligned}$$

$$\begin{aligned} v_2 = & A \cos \gamma_1 s_1 H e^{-\gamma_2 s_2 z} e^{-i\mu x} - iAb \sum_{m=1}^M \frac{\cos \gamma_1 \xi_{1m} H e^{-\gamma_2 s_2 z}}{v_m H} \\ & \times \left\{ e^{-i\mu y} \int_{-\infty}^x (i\mu h'_0 - s_1^2 h_0) \times e^{i(y-x)v_m} dy \right. \\ & \left. + e^{i\mu y} \int_x^{\infty} (i\theta h'_0 - s_1^2 h_0) e^{-i\theta y} \times e^{-i(y+x)v_m} dy \right\}, \quad (46) \end{aligned}$$

with $\text{Re}(v_m) > 0$.

From the consideration of the upper layer as irregular, the expressions in Equations (45)–(46) together with the function $h_0(x)$ defined in Equation (2) provide

$$\begin{aligned} v_1 = & A \cos \gamma_1 s_1 (z+H) e^{-i\mu x} - iAb \sum_{m=1}^M \frac{\cos \gamma_1 \xi_{1m}(z+H)}{v_m H} e^{iv_m x} \\ & \times \left\{ (\mu v_m + \mu^2 + s_1^2) \int_{-\frac{s}{2}}^{\frac{s}{2}} h_0 e^{-i(v_m+\mu)y} dy \right\}, \quad (47) \end{aligned}$$

$$v_2 = A \cos \gamma_1 s_1 H e^{-\gamma_2 s_2 z} e^{-i\mu x} - iAb \sum_{m=1}^M \frac{\cos \gamma_1 \xi_{1m} H e^{-\gamma_2 s_2 z}}{v_m H} \times \left\{ (\mu v_m + \mu^2 + s_1^2) \int_{-\frac{s}{2}}^{\frac{s}{2}} h_0 e^{-i(v_m + \mu)y} dy \right\}. \quad (48)$$

Equations (47) and (48) describe the non-zero displacement component of Love waves that propagate through a rough surface in a layered transversely isotropic poroelastic rock medium.

4 Particular Cases

The findings from the current analysis can be evaluated for three different surface irregularities, namely (I) a parabolic shape, (II) a triangular notch shape, and (III) a rectangular shape.

4.1 Case I: An Irregularity with a Parabolic Type Shape on the Upper Surface

The equation corresponds to the parabolic type shape irregularity in the upper surface (as shown in Figure 3) can be represented as (Chattopadhyay et al., 2010; Negi and Singh, 2019):

$$h_0(x) = \begin{cases} 0, & x > \frac{s}{2}, \text{ and } x < -\frac{s}{2} \\ \left(1 - \frac{4x^2}{s^2}\right), & -\frac{s}{2} \leq x \leq \frac{s}{2} \end{cases} \quad (49)$$

In the upper layer of transversely isotropic poroelastic structure, the propagation of the first mode of Love waves, which satisfies the periodic equation (Equation (36)) for Love waves will be considered. The substitution of $\mu = v_1$, $s_1 = \xi_{11}$; $m = 1$ (in the case of the first mode), in Equation (47) along with the use of Equation (51) provide

$$\frac{v_{1,ref}^P}{A} = ib \frac{\cos \gamma_1 \xi_{11} (z + H)}{v_1 H} e^{iv_1 x} (2v_1^2 + \xi_{11}^2) \left(\frac{2 \sin v_1 s}{s^2 v_1^3} - \frac{2 \cos v_1 s}{s v_1^2} \right) \quad (50)$$

Equation (50) presents the reflected displacement component resulting from the scattering of Love waves propagating through an irregular

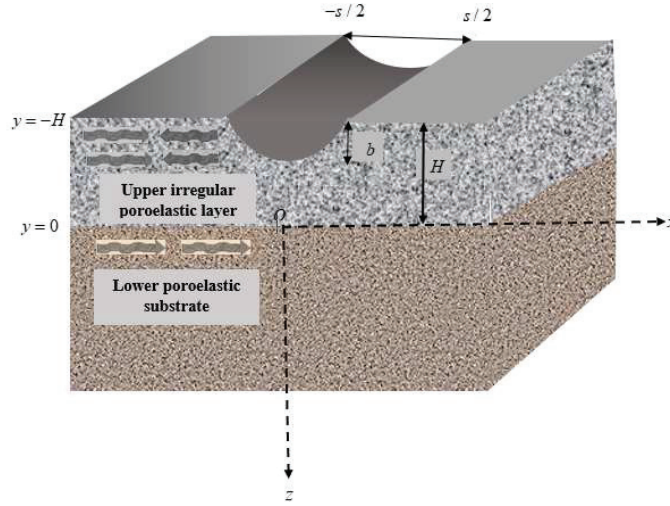


Figure 3 Parabolic type shape irregularity in upper surface.

transversely isotropic poroelastic rock structure with a parabolic-shaped irregularity on the upper surface (mentioned by the superscript P).

4.2 Case II. An Irregularity with a Triangular Notch Type Shape on the Upper Surface

The equation for the irregularity with a triangular notch shape (illustrated in Figure 4) on the upper surface can be expressed as follows (Chattopadhyay et al., 2010; Negi and Singh, 2019):

$$h_0(x) = \begin{cases} 0, & x > \frac{s}{2}, x < \frac{-s}{2} \\ 1 + \frac{2x}{s}, & \frac{-s}{2} \leq x \leq 0 \\ 1 - \frac{2x}{s}, & 0 \leq x \leq \frac{s}{2} \end{cases} \quad (51)$$

Once again, we examine the propagation of Love waves, with the condition that only the first mode of waves propagates in the upper poroelastic layer of the studied poroelastic rock structure, which also satisfies the generalized periodic equation for Love waves (Equation (36)). Using Equation (51) and also substituting $\mu = \nu_1$, $s_1 = \xi_{11}$; $m = 1$ (for first mode) in Equation (47),

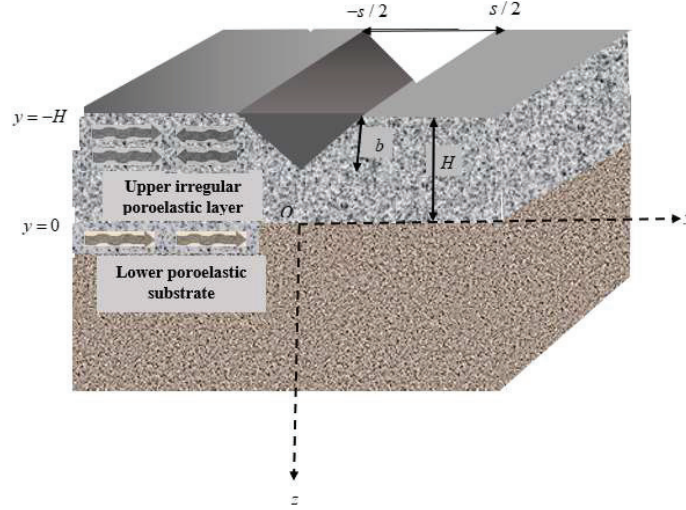


Figure 4 Triangular notch type shape irregularity in upper surface.

the component of reflected displacement resulting from the scattering of Love waves propagating through an irregular transversely isotropic poroelastic rock structure with a triangular notch-shaped irregularity on the upper surface of the studied poroelastic rock structure can be expressed as:

$$\frac{v_{1,ref}^T}{A} = ib \frac{\cos \gamma_1 \xi_{11}(z+H)}{v_1 H} e^{iv_1 x} (2v_1^2 + \xi_{11}^2) \left(\frac{2 \sin^2 \frac{v_1 s}{2}}{s v_1^2} \right) \quad (52)$$

The superscript “T” pertains to the irregularity with a triangular notch-shaped form on the upper surface of the studied structure.

4.3 Case III. An Irregularity with a Rectangular-shaped Form on the Upper Surface

The irregularity with a rectangular-shaped form on the upper surface of the studied poroelastic structure (shown in Figure 5) can be described using the following equation (Negi and Singh, 2019):

$$h_0(x) = \begin{cases} 0, & x > \frac{s}{2}, x < \frac{-s}{2} \\ 1, & \frac{-s}{2} \leq x \leq \frac{s}{2} \end{cases} \quad (53)$$

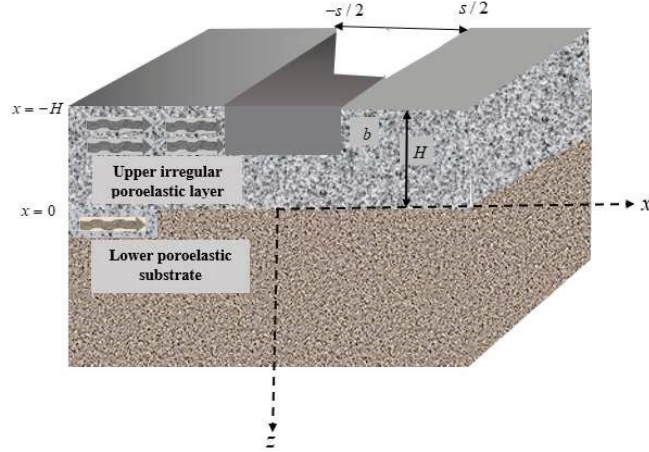


Figure 5 Rectangular type shape irregularity in upper surface.

We assume that the propagation of the first mode of Love waves satisfies the generalized equation for periodic Love waves (Equation (36)). By utilizing Equation (53) and substituting $\mu = v_1$, $s_1 = \xi_{11}$; $m = 1$ (for the first mode) in Equation (47), the component of reflected displacement in an irregular transversely isotropic poroelastic rock medium containing surface irregularity of rectangular type shape can be expressed as

$$\frac{v_{1,ref}^R}{A} = ib \frac{\cos \gamma_1 \xi_{11}(z + H)}{v_1 H} e^{iv_1 x} (2v_1^2 + \xi_{11}^2) \left(\frac{\sin v_1 s}{v_1} \right) \quad (54)$$

In Equation (54), irregularity in the upper surface of studied poroelastic structure is indicated by the superscript ‘‘R’’.

5 Results Validation

5.1 Verification of the Dispersion Relation

If $c_{44}^1 = c_{66}^1 = \mu_1$, $c_{44}^2 = c_{66}^2 = \mu_2$, then the relation representing the dispersion characteristics of Love waves in Equation (36) convert to

$$\tan \sqrt{\left(\frac{c_{ph}^2}{\beta_1^2} - 1 \right)} vH = \frac{\mu_2 \sqrt{\left(1 - \frac{c_{ph}^2}{\beta_2^2} \right)}}{\mu_1 \sqrt{\left(\frac{c_{ph}^2}{\beta_1^2} - 1 \right)}}, \quad (55)$$

In Equation (55), μ_1 and μ_2 represent the shear modulus of upper isotropic elastic layer and half-space respectively. The expression in Equation (55) represents the exactly same form as the classical equation for the Love wave (Love, 1944).

5.2 The Upper Surface Irregularity Characterized by a Parabolic Shape Results in a Reflected Displacement

For the case of $c_{44}^1 = c_{66}^1$ i.e. $\gamma_1 = \sqrt{\frac{c_{44}^1}{c_{66}^1}} = 1$, Equation (52) reduces to

$$\frac{v_{1,ref}^P}{A} = ib \frac{\cos \xi_{11}(z + H)}{vH} e^{ivx} (2v^2 + \xi_{11}^2) \left(\frac{2 \sin vs}{s^2 v^3} - \frac{2 \cos vs}{sv^2} \right). \quad (56)$$

Equation (56) provides the closed-form expression for the non-vanishing component of reflected displacement induced during the interaction of irregular upper surface and propagating Love waves in the upper layer of the layered isotropic elastic structure. In Equation (56), the closed-form expression for reflected displacement has the similar form as provided by Chattopadhyay et al. (2010) by reducing the viscoelastic case to isotropic and also provided by Wolf (1970) in the isotropic elastic structure.

5.3 The Upper Surface Irregularity Characterized by a Triangular Notch Shape Results in a Reflected Displacement

Similarly, after substituting the values $\gamma_1 = \sqrt{\frac{c_{44}^1}{c_{66}^1}} = 1$, and $v_r = v_1$, in Equation (52), we have

$$\frac{v_{1,ref}^T}{A} = ib \frac{\cos \xi_{11}(z + H)}{vH} \times e^{ivx} (2v^2 + \xi_{11}^2) \left(\frac{2 \sin^2 \frac{vs}{2}}{sv^2} \right). \quad (57)$$

Equation (57) adduces the expression of the component of the displacement caused by reflected Love waves propagating through the irregular upper surface of an isotropic elastic structure having triangular notch type shape irregular surface. The expression mention in Equation (57) is found to be well matches with the results by Chattopadhyay et al. (2010) by reducing the viscoelastic case to isotropic and also provided by Wolf (1970) for the isotropic case.

6 Numerical Results and Discussion

In order to compute numerically and illustrate graphically the phase velocity of scattered Love waves and the component of the displacement because of the reflected Love waves in a transversely isotropic poroelastic layer overlying a transversely isotropic poroelastic substrate, the below-mentioned physico-mechanical properties of the poroelastic rocks are considered:

- (i) Properties of the upper poroelastic rock layer (Batugin and Nirenburg, 1972)

$$c_{44}^1 = 8.30 \times 10^9 \text{ N/m}^2, \quad c_{66}^1 = 7.77 \times 10^9 \text{ N/m}^2,$$

$$\rho_1 = 2022 \text{ Kg/m}^3, \quad d_1 = \frac{d_1'}{\rho_1} = 0.8.$$

- (ii) Properties of the lower poroelastic rock material half-space (Batugin and Nirenburg, 1972; Zhang, 2004)

$$c_{44}^2 = 20.8 \times 10^9 \text{ N/m}^2, \quad c_{66}^2 = 21.3 \times 10^9 \text{ N/m}^2,$$

$$\rho_2 = 2700 \text{ Kg/m}^3, \quad d_2 = \frac{d_2'}{\rho_2} = 0.9.$$

If not else explained:

$$(y + H)/H = 10, \quad x/H = 10, \quad s/H = 0.01, \quad b/H = 0.001.$$

The dimensionless phase velocity and induced reflected mechanical displacement caused by Love waves scattering in the upper irregular surface of the transversely isotropic poroelastic rock medium are illustrated by Figures 6(a) to 10.

Figure 6(a) depicts the efficacy of the anisotropic parameter on the dimensionless phase velocity of the scattered Love waves. From the observation of Figure 6(a), it is noticed that the increase in the anisotropy (associated with the shear modulus) of upper poroelastic layer in the studied rock structure leads to the decreasing velocity (corresponds to phase) of the scattered Love waves.

The influence of porosity parameter on the dimensionless phase velocity has been portrayed through Figure 6(b). It has been examined from Figure 6 that with the increase in the porosity parameter i.e. porosity decreases, the phase velocity of the scattered Love waves decreases.

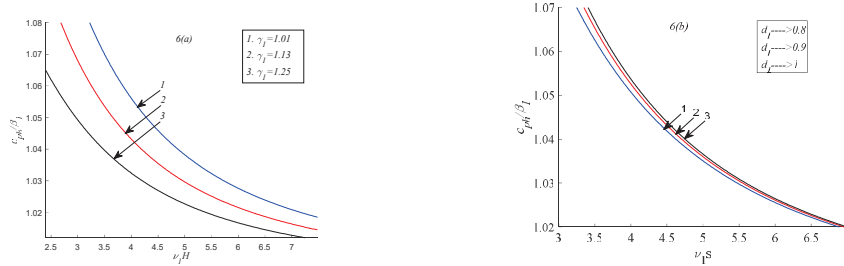


Figure 6 Variation of the scaled phase velocity (c_{ph}/β_1) against scaled wave number ($v_1 H$) for the distinct values of (a) anisotropy parameter ($\gamma_1 = \sqrt{c_{66}^1/c_{44}^1}$) and (b) porosity parameter (d_1) corresponds to the upper poroelastic rock layer in the studied transversely isotropic poroelastic rock structure.

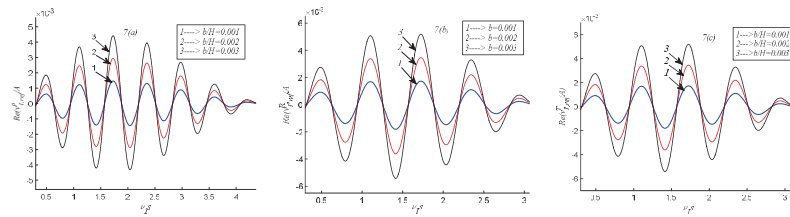


Figure 7 Dimensionless induced reflected displacement against dimensionless width ($v_1 s$) for different vertical irregularity parameter (b/H) for different cases viz. (a) parabolic type shape irregularity in upper surface [$\text{Re}(v_{1,\text{ref}}^P/A)$]; (b) rectangular type shape irregularity in upper surface [$\text{Re}(v_{1,\text{ref}}^R/A)$]; (c) triangular notch type shape irregularity in upper surface [$\text{Re}(v_{1,\text{ref}}^T/A)$] in the studied transversely isotropic poroelastic rock structure.

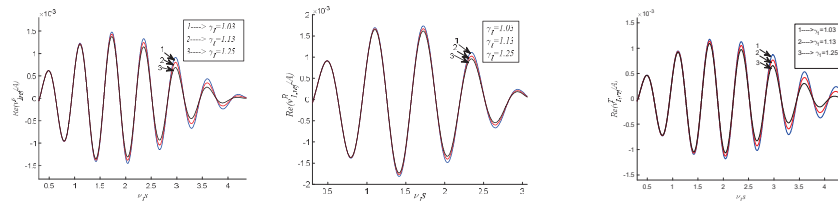


Figure 8 Dimensionless induced reflected displacement [$\text{Re}(v_{1,\text{ref}}^P/A)$] against dimensionless width ($v_1 s$) for the different anisotropic parameter (γ_1) for different cases viz. (a) parabolic type shape irregularity in upper surface [$\text{Re}(v_{1,\text{ref}}^P/A)$]; (b) rectangular type shape irregularity in upper surface [$\text{Re}(v_{1,\text{ref}}^R/A)$]; and (c) triangular notch type irregularity in upper surface [$\text{Re}(v_{1,\text{ref}}^T/A)$] in the studied transversely isotropic poroelastic rock structure.

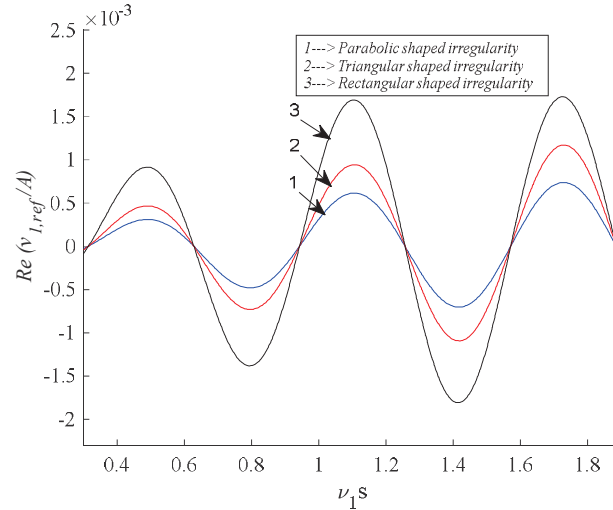


Figure 9 Dimensionless induced reflected displacement $[\text{Re}(v_{1,\text{ref}}/A)]$ against scaled vertical depth ($v_1 s$) for different physical scenarios of the irregularity in upper surface viz. parabolic type shape, triangular notch type shape, and rectangular type shape in the studied transversely isotropic poroelastic rock structure.

The effectiveness of the vertical irregularity parameter (which is linked to the depth of an irregularity on the upper rough surface), in influencing the induced reflected displacement is shown in Figures 7(a), 7(b), and 7(c) for different irregular shapes: parabolic, rectangular, and triangular notch, respectively. These figures demonstrate that increasing the value of the vertical irregularity parameter results in an increase in the induced reflected displacement for all three surface irregularity shapes studied.

Figures 8(a), 8(b), and 8(c) demonstrate the impact of the anisotropic parameter, which is linked to the shear modulus, on the reflected displacement for different types of irregularities in the upper surface. These irregularities include shapes such as parabolic, rectangular, and triangular notch. The observation of these figures provides that as the anisotropic parameter of the upper layer increases (anisotropy of upper layer prevails), the component of reflected displacement induced because of Love waves scattering decreases for all considered cases of irregularity in upper surface.

The comparative analysis of parabolic type shape, rectangular type shape, and triangular notch type shape irregularity in upper surface has been accomplished through Figure 9. From the analysis of Figure 9, it is found that the component of the induced reflected displacement attains maximum value

for the situation when irregularity in upper surface is of rectangular type shape while it becomes minimum for the situation when irregularity in upper surface is of parabolic type shape. It is also examined that the component of reflected displacement for the remaining situation (i.e. in the situation when the upper surface has the irregularity of triangular notch type shape) lies between its value for the above two cases.

7 Concluding Remarks

The phenomena of the Love waves propagation through the irregularity in the upper poroelastic surface of transversely isotropic poroelastic rock composite structure has been studied through the present mathematical problem. The problem has been dealt with the help of analytical procedure. The closed form expressions for the dispersion relation (associated with the phase velocity) and also the component of reflected displacement are derived. Observations have been made on the effectuality of anisotropy parameter and porosity parameter on the phase velocity of Love waves. The present study has also investigated the impact of the vertical irregularity parameter and anisotropic parameter on the reflected displacement. Additionally, the following results can be considered as the main findings of this research:

1. The phase velocity corresponds to the Love waves because of the scattering phenomena degrades with the increase of anisotropy in the studied poroelastic rock structure.
2. Scattering causes an increase in the phase velocity of Love waves when the porosity of the upper poroelastic rock layer is reduced.
3. Reflected displacement induced because of the Love waves scattering decreases with the increase in the anisotropic parameter (associated with the shear modulus) for all studied shapes of irregularity in upper surface.
4. For all the irregular surface shapes studied, an increase in the induced reflected displacement occurs as the vertical irregularity parameter increases.
5. The displacement induced due to reflected Love waves for the situation when the irregularity of rectangular type shape is in upper surface is maximum while its value becomes minimum when the situation of parabolic type shape irregularity is considered in upper surface. Moreover, the displacement because of reflected Love waves for the triangular notch shaped irregularity in the upper surface falls between the values obtained for the other two types of irregularities discussed earlier.

Acknowledgement

The authors convey their sincere gratitude to VIT-AP University for providing the research facilities to accomplish the current research paper.

Disclosure Statement

The authors reported no potential competing interest.

Data Availability

All the data used in this study have been provided as well as cited in the manuscript.

Appendix

$$\gamma_1 = \sqrt{\frac{c_{44}^1}{c_{66}^1}}, \gamma_2 = \sqrt{\frac{c_{44}^2}{c_{66}^2}}, \beta_1^2 = \frac{c_{44}^1}{\rho_1'}, \beta_2^2 = \frac{c_{44}^2}{\rho_2'}, K_1^2 = \frac{\omega^2}{\beta_1^2}, K_2^2 = \frac{\omega^2}{\beta_2^2},$$

$$\Gamma_0(v) = \frac{\{\lambda \cos \gamma_1 \xi_1 z - i \sin \gamma_1 \xi_1 z\} e^{+ivy-ivx}}{(i \cos \gamma_1 \xi_1 H - \lambda \sin \gamma_1 \xi_1 H) \xi_1},$$

$$\Gamma_{00}(v) = \frac{\lambda e^{-\gamma_2 \xi_2 z} e^{+ivy-ivx}}{(i \cos \gamma_1 \xi_1 H - \lambda \sin \gamma_1 \xi_1 H) \xi_1},$$

$$R_{12} = \frac{c_{66}^2}{c_{66}^1}, \gamma_1 = \sqrt{\frac{c_{44}^1}{c_{66}^1}}, \gamma_2 = \sqrt{\frac{c_{44}^2}{c_{66}^2}}, \beta_1^2 = \frac{c_{44}^{1R}}{d_1'}, \beta_2^2 = \frac{c_{44}^{2R}}{d_2'},$$

References

- Biot, M. A. (1956). Theory of propagation of elastic waves in a fluid-saturated porous solid. I. Low-frequency range. *The Journal of the Acoustical Society of America*, 28(2), 168–178. URL: <https://asa.scitation.org/doi/abs/10.1121/1.1908241>.
- Biot, M. A. (1962). Mechanics of deformation and acoustic propagation in porous media. *Journal of Applied Physics*, 33(4), 1482–1498. URL: <https://aip.scitation.org/doi/abs/10.1063/1.1728759>.

- Chattopadhyay A, De RK (1983). Love waves in a porous layer with irregular interface. *Int J Eng Sci* 21(11):1295–1303. URL: <https://www.sciencedirect.com/science/article/abs/pii/002072258390126X>.
- Chattopadhyay, A., and A.K. Pal (1982). SH waves in anisotropic layer with irregular boundary. *Bull. Acad. Pol. Sci.* 30, 51–59.
- Chattopadhyay, A., Gupta, S., Sharma, V. K., & Kumari, P. (2010). Propagation of shear waves in viscoelastic medium at irregular boundaries. *Acta Geophysica*, 58(2), 195–214. URL: <https://link.springer.com/article/10.2478/s11600-009-0060-3>.
- El Baroudi, A. (2018). Influence of poroelasticity of the surface layer on the surface love wave propagation. *Journal of Applied Mechanics*, 85(5), 051002. URL: <https://asmedigitalcollection.asme.org/appliedmechanics/article-abstract/85/5/051002/422540/Influence-of-Poroelasticity-of-the-Surface-Layer>.
- Love, A. E. H. (1944). A treatise on the mathematical theory of elasticity, Dover Publications. *New York*, 1.
- Negi, A., and Kumar Singh, A. (2019). Analysis on scattering characteristics of Love-type wave due to surface irregularity in a piezoelectric structure. *The Journal of the Acoustical Society of America*, 145(6), 3756–3783. URL: <https://asa.scitation.org/doi/abs/10.1121/1.5102165>.
- Wolf, B. (1970). Propagation of Love waves in layers with irregular boundaries. *Pure and Applied Geophysics*, 78(1), 48–57.

Biographies



Anil Negi is working as an Assistant Professor in Department of Mathematics, School of Advanced Sciences, VIT-AP, University. He completed his M.Sc. in Mathematics & Computing and Ph.D. in Applied Mathematics, from IIT(ISM), Dhanbad, Jharkhand, India. He is an editorial board member and

reviewer in international journals. He has published 10 research publications in international SCI-indexed journals of repute. His fields of research are computational solid mechanics, geomechanics, theoretical seismology, elastodynamics, piezoelectricity, fracture mechanics, etc. He is a life member of the international society International Association of Engineers (IAENG). He is also affiliated with the reputed Indian society such as Indian Mathematical Society and Indian Science Congress.



Saurabh Kapoor working as an Assistant Professor of Mathematics in NCERT and presently posted at RIE Bhubaneswar. He received his Ph.D. in Mathematics from IIT Roorkee in 2015. His research areas are computational fluid dynamics (CFD), hydrodynamics stability, and Finite element method. He published more than 40 articles in National and International peer reviewed journals. He also published two book chapters in the CRC press book. Dr. Kapoor also visited more than three countries for the research work. He also handled more than five research projects and presently guiding four Ph.D. students in Applied Mathematics. He is a member of various international societies such as International Association of Computer science and Information Technology (IACSIT), International association of Engineers (IAEG), International Innovative Scientific and Research Organization. He is also the member of reputed Indian Societies such as Indian Society of Bio mechanics, Indian Society of Heat and Mass Transfer (ISHMT), and Odisha Mathematical Society.